

Fundamental Study of Carbon Materials Derived from Empty Fruit Bunch via Hydrothermal Carbonization

Kanogpan GUNTAGERNG¹, Gasidit PANOMSUWAN² and Apiluck EIAD-UA^{1,*}

¹*College of Nanotechnology, King Mongkut's Institute of Technology Ladkrabang, Bangkok 10520, Thailand*

²*Department of Materials Engineering, Faculty of Engineering, Kasetsart University, Bangkok 10900, Thailand*

(* Corresponding author's e-mail: apiluck.ei@kmitl.ac.th)

Received: 31 October 2017, Revised: 23 January 2018, Accepted: 5 March 2018

Abstract

The utilization of biomass has recently gained great attention in recent years owing to growth of global environmental concerns. The aim of this work is to study the morphology of carbon materials derived from biomass oil palm empty fruit bunch (EFB) via hydrothermal carbonization (HTC) at different temperatures (160 - 200 °C) and times (4 - 12 h) followed by carbonization at 300 - 900 °C under nitrogen atmosphere for 2 h. The physiochemical properties of carbon sample were characterized by scanning electron microscopy (SEM), Fourier transform infrared spectroscopy (FTIR), Raman spectroscopy and surface area analysis. The results demonstrated that the increase of hydrothermal temperature, hydrothermal time, and carbonization temperature resulted in the formation of carbon materials with higher surface area, porosity and carbon content. Our results revealed that carbon derived from EFB via HTC at optimal condition exhibited porous structure with high surface area, which can be further applied for absorbent applications.

Keywords: Biomass, empty fruit bunch, hydrochar, hydrothermal carbonization

Introduction

Lignocellulosic biomass materials are derived from a variety of plants, agricultural crop residues and animals, such as husk [1], wheat straw [2] and bagasse [3]. Moreover, they are renewable sources of energy that can help in improving environment, economy and energy security [4]. Thailand is an agricultural country that produces a large amount of biomass residues every day. Among several agricultural products, oil palm is one of the major economic crops in Thailand. Empty fruit bunch (EFB) is the major waste product in oil palm industry. Therefore, it would be worth if we can find the effective strategy to increase the value of oil palm wastes by converting them to higher-value added product like carbon materials.

Hydrothermal carbonization (HTC) is a thermochemical conversion process from biomass into smokeless, high carbon content and more valuable products (i.e., solid fuel) [5]. The HTC is usually performed at temperatures ranging from 180 - 280 °C and pressures higher than water saturation pressure to against water into liquid state, under an inert atmosphere. Reaction time has been reported in a broad range from 1 min to several hours [6]. Additives, such as acids or bases, can also affect the formation of carbons, which are then physically or chemically activated to obtain carbons with high porous structure [7].

Selected papers from The 1st MRS Thailand Conference, October 31st - November 3rd, 2017

In this work, EFB was employed as a precursor in the synthesis of carbon materials via HTC process. The temperature and time used in hydrothermal reaction were varied in the range of 160 - 180 °C and 4 - 12 h, respectively. The best hydrothermally treated samples were selected for subsequent carbonization at 300 - 900 °C for 2 h under nitrogen atmosphere. The effects of hydrothermal and carbonization conditions on the properties of carbons synthesized were characterized by several techniques, including scanning electron microscopy (SEM), Fourier transform infrared spectroscopy (FTIR), X-ray diffraction (XRD), Raman spectroscopy and surface area analysis.

Materials and methods

Preparation of carbon materials from EFBs via HTC

EFBs were obtained from the Krabi province of the Southern Thailand. Prior to use, EFBs were dried at 90 °C overnight and then reduced their size by using a blender machine, followed by sieving with a 700 µm mesh. 10 g of grinded EFBs was mixed with 100 mL of DI water and transferred into a Teflon-lined stainless-steel reactor. The hydrothermal reaction was performed at different temperatures (i.e., 160, 180, and 200 °C) and times (i.e., 4, 8, and 12 h). Subsequently, the resultant hydrochars were quenched in water and dried at 90 °C overnight. The experimental conditions and the respective samples prepared are shown in **Table 1**. The best hydrochar sample obtained from hydrothermal process was selected and carbonized at 300 - 900 °C for 2 h under N₂ flow. **Figure 1** displays a scheme of the synthesis procedure of carbon materials derived from EFBs via HTC.

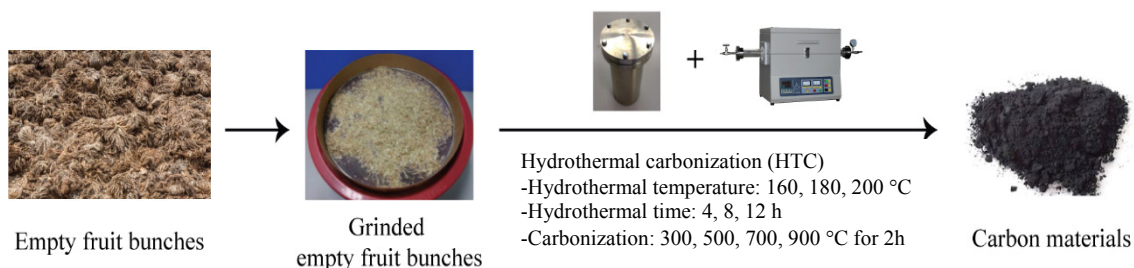


Figure 1 Scheme showing the synthesis procedure of carbon materials derived from EFBs via HTC.

Table 1 Experimental conditions for hydrothermal process.

Condition	Temperature (°C)	Time (h)
1	160	4
2	160	8
3	160	12
4	180	4
5	180	8
6	180	12
7	200	4
8	200	8
9	200	12

Characterization

The proximate and ultimate analyses were carried out to evaluate the chemical and elemental compositions of EFBs according to the standard method [8]. SEM images were taken on a Zeiss EVO 50 microscope operated at an accelerating voltage of 10 kV. The presence of functional group on carbon samples were confirmed with a Thermo Scientific Nicolet 6700 FTIR spectrometer. N₂ adsorption-

desorption isotherms were measured on a 3Flex Micromeritics surface analyzer at liquid N₂ temperature (−196 °C) to investigate specific surface area, pore volume and pore size distribution of the catalysts. Prior to the measurement, all samples were degassed at 150 °C for 6 h under vacuum. The specific surface area was determined by the Brunauer-Emmett-Teller (BET) method at relative pressures (p/p_0) between 0.05 and 0.30. The pore volume and pore size distribution were determined by the Barrett-Joyner-Halenda (BJH) method. XRD patterns were recorded on a Philips X'Pert PRO MPD diffractometer operated at 40 kV and 30 mA with monochromatic Cu K α radiation ($\lambda = 0.154$ nm). Raman spectra were recorded on a Thermo Scientific DXR SmartRaman spectrometer with a laser-excitation wavelength of 532.1 nm.

Results and discussion

The results of proximate and ultimate analyses of EFB are shown in **Table 1**. It was found that as-received EFB was mainly composed of moisture of 63.49 ± 0.53 wt% and volatile of 32.56 ± 0.24 wt% as two major components, while fixed carbon and volatile were found to be only 2.96 ± 0.08 and 1.00 ± 0.04 wt%, respectively. In case of EFBs after drying, C, H, N and O obtained from elemental analysis were 43.78 ± 0.05 , 6.06 ± 2.02 , 0.56 ± 0.01 and 49.67 ± 0.04 wt%, respectively.

The SEM images of EFB and hydrochars are shown in **Figure 2**. It was clearly observed the significant difference in morphology of hydrochars hydrothermally treated at different temperatures and times. Hydrochars derived from hydrothermal process at 160, 180 and 200 °C showed rougher surfaces with more rupturing structure as compared to EFB, which suggests the decomposition of the lignocellulosic structure of EFB [9,10].

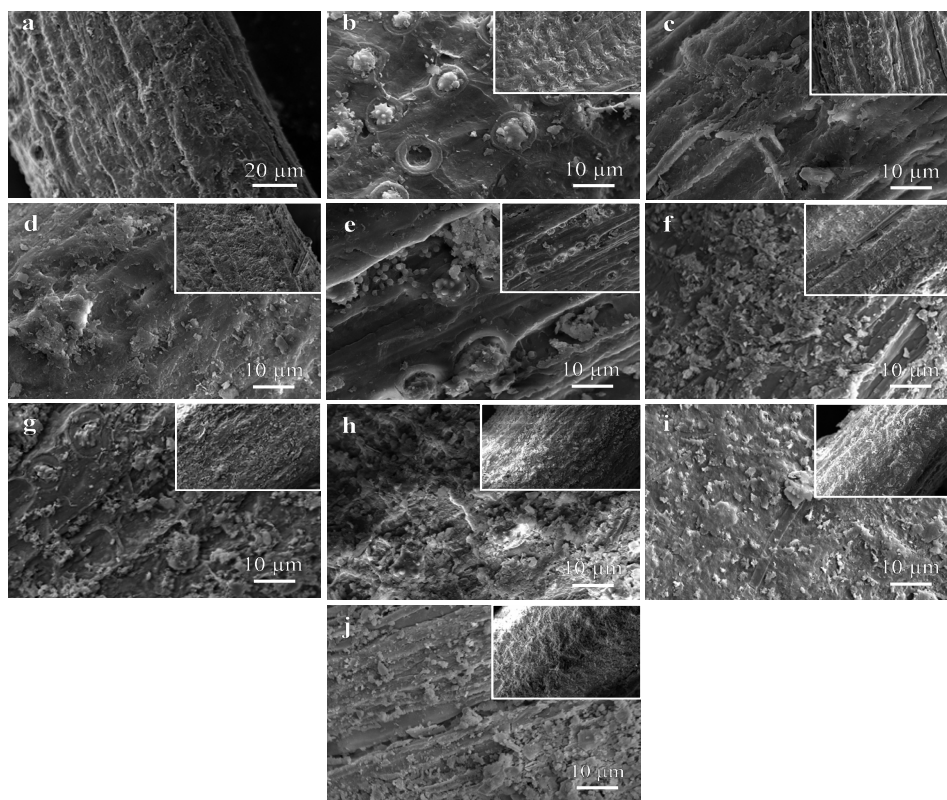


Figure 2 (a) SEM images (500 \times) of EFB. SEM images (1000 \times) of EFB hydrothermally treated at different conditions: (b) 160 °C for 4 h, (c) 160 °C for 8 h, (d) 160 °C for 12 h, (e) 180 °C for 4 h, (f) 180 °C for 8 h, (g) 180 °C for 12 h, (h) 200 °C for 4 h, (i) 200 °C for 8 h and (j) 200 °C for 12 h.

To identify the presence of functional groups, the FTIR spectra of EFB and hydrochars after hydrothermal at 200 °C for 4, 8 and 12 h were collected and are shown in **Figure 3**. A broad absorption band at 3000 - 3600 cm^{-1} and a small sharp peak at 2850 - 2950 cm^{-1} are attributed to stretching vibration of OH (hydroxyl) and C-H stretching vibration, respectively. The absorption bands at 1620 and 1720 cm^{-1} are attributed to C=O and C=C functional groups in aromatic structure, respectively. The bands in the range of 1250 - 1350 cm^{-1} suggests the presence of C-O and OH bending vibrations. In addition, the emergence of bands at between 950 and 1000 cm^{-1} is assigned to C-H vibration in aromatic structure [11-14]. As the hydrothermal time increased, the peak of C-H stretching vibration and C-H vibration in aromatic structure decreased progressively, whereas other absorption peaks were almost unchanged.

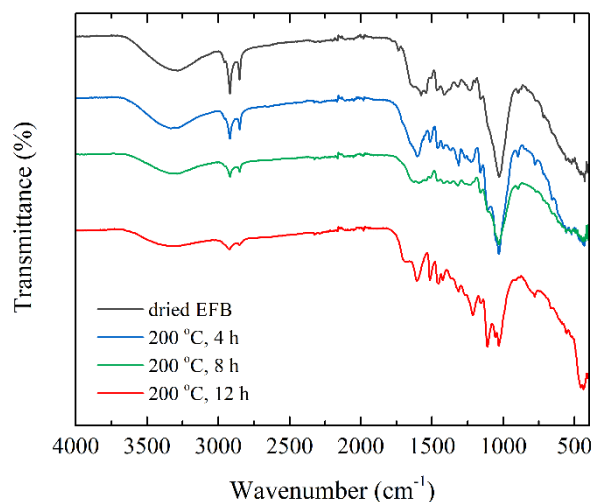


Figure 3 FTIR spectra of: (a) EFB and hydrochars derived from hydrothermal process at 200 °C for 4, 8 and 12 h.

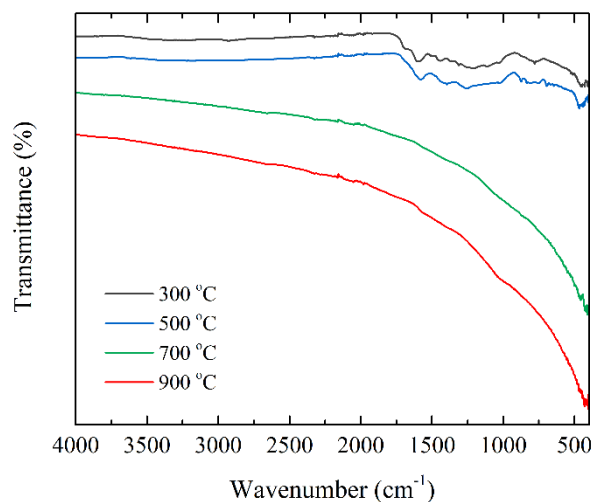


Figure 4 FTIR spectra of hydrochars derived from hydrothermal process at 200 °C for 12 h after carbonization at 300, 500, 700 and 900 °C for 2 h.

The hydrochar obtained from hydrothermal process at 200 °C for 12 h was selected for further carbonization process owing to its most rough and rupturing surface. **Figure 4** present the FTIR spectra of hydrochars after carbonization at different temperatures. As can be seen, all absorption bands decreased significantly with increasing temperature. The FTIR spectra became featureless at carbonization temperature of 700 °C. The disappearance of absorption bands at 1000 - 1600 cm^{-1} and 3000 - 3600 cm^{-1} indicated that decarboxylation and dehydration occurred during carbonization, respectively [15]. According to the FTIR results, it allows us to conclude that carbonization at high temperatures under inert atmosphere could lead to a strong reduction of the oxygen content through decomposition of functional groups.

The XRD measurement was investigated to examine the phase structure of carbon materials carbonized at different temperatures, as shown in **Figure 5a**. It should be noted that the sharp diffraction peaks at 37.9° and 44.1° and a small peak at 64.5° were originated from an Al holder used in the measurement, which is not related to the samples. The broad diffraction at 2 θ angle around 20 - 30° was evidently noticed for all carbon samples, corresponding to the carbon. The broad characteristic feature indicates the major presence of amorphous phase. As the carbonization temperature increased, the (002) diffraction peak of carbon phase became narrower. In addition, a significant shift of the 002 peak from 21.1° to 24.4° was also observed. The d_{002} lattice spacing of carbons carbonized at 900 °C was estimated to be about 0.364 nm, which was lower than that of ideal graphite (0.335 nm). The shift of the 002 peak to higher 2 θ angle concomitant with its narrower feature are evidence that the carbon samples were more graphitized and the size of crystalline graphite was larger at high carbonization temperatures.

To further evaluate more detailed information on the structure of carbons, Raman spectroscopic analysis was carried out, as shown in **Figure 5b**. The Raman spectra of carbonized samples was comprised of two pronounced peaks centered at 1360 and 1600 cm^{-1} , which are related with the D band and G band, respectively. The D band is related to the breaking of symmetry caused by structural disorders and defects, whereas the G band refers to the in-plane bond stretching motion of the pair of sp^2 carbon atoms [16,17]. These two characteristic peaks had low intensity with broad feature at carbonization temperature of 300 - 700 °C, indicating an amorphous nature of carbons. Additionally, it was evidently seen that the intensity of both D and G bands increased significantly at 900 °C. This result confirmed that high carbonization temperature could lead to more graphitization of carbon samples, which are in accordance with aforementioned XRD results.

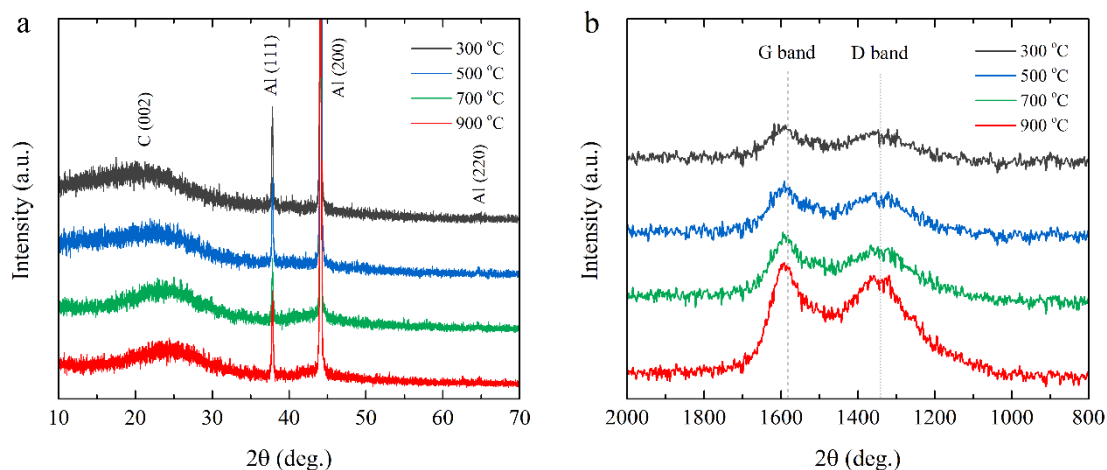


Figure 5 (a) XRD patterns and (b) Raman spectra of hydrochars carbonized at 300, 500, 700 and 900 for 2 h.

Furthermore, surface area, pore volume, and pore diameter of hydrochars carbonized at different temperatures were examined using N₂ adsorption-desorption isotherm. For the hydrochars carbonized at 300, 500 and 700 °C, their surface area were found to be very low about 3 m²/g. The low surface area of carbonized hydrochars suggests that pore structure was not developed at low carbonization temperatures. However, the surface area abruptly increased to 190 m²/g when carbonization was done at 900 °C, confirming that high carbonization temperature of 900 °C is greatly required for the pore development. The N₂ adsorption-desorption isotherms of hydrochar carbonized at 900 °C is displayed in **Figure 6**. It exhibited type II isotherms with a hysteresis feature, indicating its hierarchical pore structure, including micro-, meso and macropores. From the *t*-plot, the micropore and external (meso and macropores) surface areas were estimated to be 141.4 and 48.3 m²/g, respectively. This result indicates that the surface area of such carbon sample is mainly contributed by micropores (74.6 %), while the meso and macropores are minor contribution (35.4 %). The surface area, mean pore size and pore volume of all samples are summarized in **Table 2**. Although surface area obtained in this study is still relatively low when compared to other works, there are a plenty of room for further improvement by combination with thermal and chemical activation method [18].

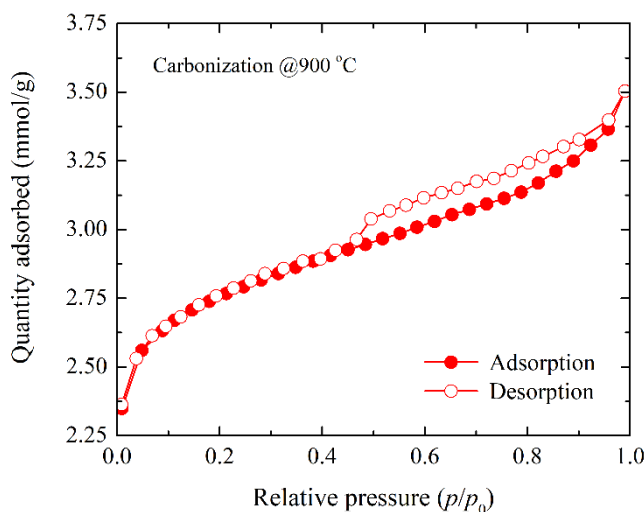


Figure 6 N₂ adsorption-desorption isotherms of hydrochar carbonized at 900 °C.

Table 2 Experimental BET data of hydrochars carbonized at 300, 500, 700 and 900 °C.

Sample	Surface area (m ² /g)	Mean pore size (nm)	Pore volume (cm ³ /g)
EFB-300	3.3	10.2	0.006
EFB-500	3.0	11.9	0.006
EFB-700	2.6	27.6	0.007
EFB-900	189.7	31.7	0.039

Conclusions

The reaction temperature and time in HTC process are the significant factors in controlling physicochemical properties of carbon products. The FTIR spectra confirmed that the functional groups on hydrochars decreased as the carbonization temperature increased. The disappearance of functional groups in hydrochars was evidenced that both dehydration and decarboxylation occurred during carbonization. The XRD and Raman spectroscopy data showed that carbons became more graphitized at high carbonization temperature; however, they were mainly composed of amorphous phase. Among a series of conditions investigated, we found that hydrothermal process at 200 °C for 12 h and further carbonization at 900 °C for 2 h is an optimal condition to obtain hierarchically porous carbon with surface area as high as 190 m²/g. We anticipate that carbon materials prepared from EFB via HTC at optimal HTC condition can be further applied for absorbent applications.

Acknowledgements

The authors are thankful to the College of Nanotechnology, King Mongkut's Institute of Technology Ladkrabang and Department of Materials Engineering, Faculty of Engineering, Kasetsart University for supporting this work.

References

- [1] D Kalderis, MS Kotti, A Méndez and G Gasco. Characterization of hydrochars produced by hydrothermal carbonization of rice husk. *Solid Earth* 2014; **5**, 477-83.
- [2] M Toufiq Reza, J Mumme and A Ebert. Characterization of hydrochar obtained from hydrothermal carbonization of wheat straw digestate. *Biomass Convers. Biorefin.* 2015; **5**, 425-32.
- [3] MT Reza, X Yang, CJ Coronella, H Lin, U Hathwaik, D Shintani, BP Neupane and GC Miller. Hydrothermal carbonization (HTC) and pelletization of two arid land plants bagasse for energy densification. *ACS Sustain. Chem. Eng.* 2016; **4**, 1106-14.
- [4] HS Kambo and A Dutta. A comparative review of biochar and hydrochar in terms of production, physico-chemical properties and applications. *Renew. Sustain. Energ. Rev.* 2015; **45**, 359-78.
- [5] HPS Abdul Khalil, MS Alwani, R Ridzuan, H Kamarudin and A Khairul. Chemical composition, morphological characteristics, and cell wall structure of Malaysian oil palm fibers. *Polym. Plast. Tech.* 2008; **47**, 273-80.
- [6] M Toufiq Reza, A Janet, W Bejamin, B Daniela, P Judith, GL Joan and M Jan. Hydrothermal carbonization of biomass for energy and crop production. *Bioenerg. Res.* 2014; **1**, 11-29.
- [7] S Nizamuddin, S Shrestha, S Athar, B Si Ali and MA Siddiqui. A critical analysis on palm kernel shell from oil palm industry as a feedstock for solid char production. *Rev. Chem. Eng.* 2015; **32**, 489-505.
- [8] SS Jamari and JR Howse. The effect of the hydrothermal carbonization process on palm oil empty fruit bunch. *Biomass Bioenerg.* 2012; **47**, 82-90.
- [9] AB Fuertes, MC Arbestain, M Sevilla, JA Macia-Agullo, S Fiol, R Lopez, RJ Smernik, WP Aitkenhead, F Arce and F Macias. Chemical and structural properties of carbonaceous products obtained by pyrolysis and hydrothermal carbonisation of corn stover. *Aust. J. Soil Res.* 2010; **48**, 618-26.
- [10] AT Mursito, T Hirajima, K Sasaki, Upgrading and dewatering of raw tropical peat by hydrothermal treatment. *Fuel* 2010; **89**, 635-41.
- [11] T Kubilay, K Selhan, B Sema. A review of hydrothermal biomass processing. *Renew. Sust. Energ. Rev.* 2014; **40**, 673-87.
- [12] W Lili, G Yupeng, Z Yanchao, L Ying, Q Yuning, R Chunguang, M Xiaoyu and W Zichen. A new route for preparation of hydrochars from rice husk. *Biores. Tech.* 2010; **101**, 9807-10.
- [13] W Ru, L Guoqiang, L Min, Z Jianchun and H Xinmin. Preparation and N₂, CO₂ and H₂ adsorption of super activated carbon derived from biomass source hemp (*Cannabis sativa L.*) steam. *Micropor. Mesopor. Mater.* 2012; **158**, 108-16.

- [14] K Ganesh, S Parshetti, H Kent and B Rajasekhar. Chemical structural and combustion characteristics of carbonaceous products obtained by hydrothermal carbonization of palm empty fruit bunches. *Biores. Tech.* 2013; **135**, 683-9.
- [15] LL Wang, YP Guo, B Zou, CG Rong, XY Ma, YN Qu, Y Li and ZC Wang. High surface area porous carbons prepared from hydrochars by phosphoric acid activation. *Biores. Tech.* 2010; **102**, 1947-950.
- [16] J Schwan, S Ulrico, V Batori and H Ehrhardt. Raman spectroscopy on amorphous carbon films. *J. Appl. Phys.* 1996; **80**, 440-7.
- [17] M Sevilla, AB Fuertes, The production of carbon materials by hydrothermal carbonization of cellulose. *Carbon* 2009; **47**, 2281-9.
- [18] M Sevilla, AB Fuertes and R Mokaya. High density hydrogen storage in superactivated carbons from hydrothermally carbonized renewable organic materials. *Energ. Environ. Sci.* 2011; **4**, 1400-10.